Back to the deformation and Stress Change Modeling home page

J. Lin and R. S. Stein,
Coseismic folding, earthquake recurrence, and the 1987 source mechanism at Whittier Narrows, Los Angeles Basin, California, *Journal of Geophysical Research, 94, pp. 9614-9632, 1989.*
[Online article] [Appendix] [Table 3A]

Coseismic Folding, Earthquake Recurrence, and the 1987 Source Mechanism at Whittier Narrows, Los Angeles Basin, California

Jian Lin

Now at: Woods Hole Oceanographic Institution, Woods Hole, Massachusetts

Ross S. Stein

US Geological Survey, Menlo Park, California

Static deformation associated with the October 1, 1987, Whittier Narrows, California, M=6.0 earthquake was detected by geodetic elevation changes. The earthquake uplifted a 1.5-km-high Quaternary fold (the Santa Monica Mountains anticlinorium) by 50 mm but caused no fault rupture at the ground surface. This suggests that folding and faulting of the Los Angeles basin sediments are coincident and continuing. After correction for surveying errors and nontectonic subsidence, we model the 214 geodetic observations with a simple dislocation in an elastic half-space. A thrust fault with reverse slip of 1.1+-0.3 m and dipping 30 +-4°N, with an upper edge at a depth of l2+-1 km and a lower edge at 17+-l km, fits the geodetic data best and is consistent with the main shock hypocenter, fault plane solution, and initial aftershock distribution. The upper limit on the static stress drop, Deltasigma, is 17.5+-5.0 MPa (175+-50 bar, The lower limit on the geodetic moment is 10+-02 x 1025 dyne cm, in accord with seismic estimates, indicating that most of the slip took place during seismic rupture. If earthquakes of M<6 characterize the blind thrust fault on which the earthquake occurred, we estimate a 200 year repeat time at Whittier Narrows, and a 5-18 year rate of earthquake occurrence within a 150-km-long band in the northern Los Angeles basin and Santa Monica Bay to the west. The 25-year rate of historical occurrence since 1860 is less than this prediction. The deficit in moment release implies that either vigorous aseismic slip or infrequent larger earthquakes occur here.

INTRODUCTION

The October 1, 1987, Whittier Narrows, California, earthquake ruptured a largely unrecognized thrust fault at a depth in excess of 12 km. Although most active folds in the basin are concealed beneath sediments from the San Gabriel mountains, the structures have been extensively drilled for oil and gas exploration, with limited publication of industry findings [Truex, 1975]. Subsidence and structural studies of the basin suggest that a former episode of extension abruptly ended at 3-5 Ma. This was followed by N-S contraction that lead to the development of a series of E-W oriented active folds in the southern Transverse Ranges and northern Los Angeles basin [Mayer,1987]. Namson and Davis [1988] proposed that slip on deep thrust faults produced the folds, but neither the presence of such faults nor their seismic potential had been demonstrated until the advent of the Whittier Narrows earthquake.

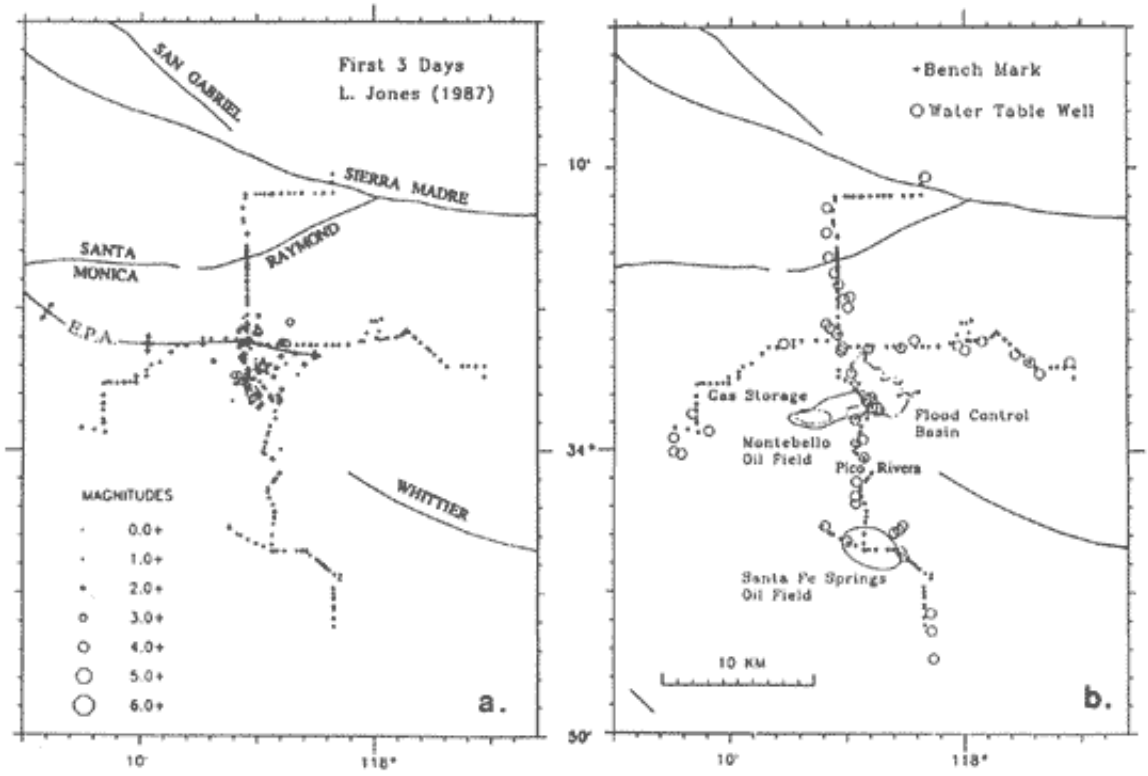

Fig 1. (a) Map showing epicentral locations of the main Whittier Narrows event of October 1, 1987, aftershocks through October 4 [after Hauksson et al. 1988], and bench marks on which elevation changes have been measured (dots). SMMA is the Santa Monica Mountains anticlinorium. (b) Location of levelling routes water wells, oil and gas fields, and the Whittier Narrow flood control basin.

Several larger earthquakes have furnished evidence that folds may grow chiefly during large earthquakes. Events that occurred beneath and uplifted actively growing anticlines include the 1964 Ms=7.5 Niigata, Japan, the 1980 Ms=7.3 El Asnam; and Algeria, the 1983 M s=6.5 Coalinga and the 1984 M s=6.1 Kettleman Hills, California, earthquakes [Stein and King, 1984]. Although smaller, the Whittier Narrows event shares this characteristic and thus raises the possibility that the principal source of future earthquakes

in the Los Angeles metropolitan area comes not from strike-slip and reverse faults prominent at the surface, but from blind (or buried) thrusts that are intimately coupled to the development of the subsurface folds. It is this question we address.

We use the geodetic record of the Whittier Narrows earthquake to resolve the earthquake source mechanism and combine this with geological data to infer an earthquake repeat time for the fault on which the event occurred. We will briefly explain the data acquisition, model the geodetic observations, and compare our source mechanism to those measured at much shorter periods from seismic radiation and to the cumulative deformation preserved by the geological structure. The data reduction and error analysis are (mercifully) relegated to a detailed appendix.

LEVELING DATA

An unusually dense geodetic network was centered on the main shock and was, coincidentally, surveyed just 20 months before the earthquake (Figure 1). The close proximity of the leveling routes to the Whittier Narrows epicentral area permits estimation of the fault geometry and coseismic slip on the fault plane, independent of the seismic and geologic data. Such serendipity is, however, tempered by leveling errors in the pre-earthquake survey that must be identified and removed and by non tectonic deformation caused by oil, gas, and water pumping in the Los Angeles basin.

The bench marks (BMs) along the 44-km-long N-S line (line 1) and the 39-km-long E-W line (line 2) were previously surveyed by the Road Department of Los Angeles County (LACO) during June-July 1965, May-July 1975, and January-February 1986 (Table 1). At the request of the U.S. Geological Survey, the National Geodetic Survey (NGS) resurveyed the lines in October and November of 1987.

The 1987-1986 elevation changes ("1987 elevations minus 1986 elevations") were obtained by subtracting the relative heights of BMs surveyed after the earthquake in 1987 from the heights of the same BM's surveyed before the earthquake in1986. The coseismic elevation changes along Line 1, in which the systematic leveling errors and non-tectonic subsidence error were removed following the procedure explained in the appendix, are shown in Figure 2a. The line 1 profile is shown with the route topography in Figure 3a. The maximum deformation of 50 mm occurs over the axis of the Santa Monica Mountains anticlinorium (formerly the Elysian Park antiform of Hauksson et al. [1988] (compare Figures 2a and 2b). The coseismic deformation along Line 2 is more subtle, with maximum deformation of 20 mm (Figure 4a).

TABLE 1. Whittier Narrows Leveling Specifications

Line	Surveyed by	Survey Period		Double or Single Run	Order of Leveling	S.D. β, mm	α,mm
Line 1	LACO	June-July	1975	single	second		1.2
	LACO	Jan.-Feb.	1986	single	second		1.2
	NGS	Oct.-N	1987	double	first	0.74	

In constructing the coseismic elevation changes in Figures 3a and 4a, we have corrected for non-tectonic subsidence during the 20-month coseismic period using the average subsidence rate observed before the earthquake during 1975-1986. By doing so, we have assumed that the rate of non-tectonic subsidence during 1975-1986 was unchanged in 1986-1987. Elevation changes during the 11-year period between 1975 and 1986 are shown

	NGS	Nov.	1987	double	first	0.74
Line 2	LACO	June-July	1975	single	second	1.2
	LACO	Jan.-Feb.	1986	single	second	1.2
	NGS	Oct.-Nov.	1987	double	first	0.74

in Figures 5a and 6a for line 1 and 2 respectively. The principal feature of the preseismic deformation on line 1 is confined subsidence in Pico Rivera, at a projected distance of 12-25 km. To assess whether groundwater fluctuations have induced the subsidence, we collected groundwater data in 55 water wells monitored by the Hydrologic Conservation Division of LACO. These wells locate within 1 km of lines 1 and 2 (Figure 1b) and were continuously monitored during the period 1975-1986; some 37 of these were also observed through late 1987. The changes in the water table during the preseismic and coseismic periods are plotted in Figures 3b and 5b for line 1 and Figures 4b and 6b for line 2. The decline in water table during 1975-1986 ranges between 0 and 4 m on Line 1 (Figure 5b) and is not well correlated with the subsidence at Pico Rivera (Figure 5a). On line 2, the water table changes are more sparse (Figures 4b and 4b), but display similar trends. We found that seasonal fluctuations in the water table generally exceed the decade-long trends.

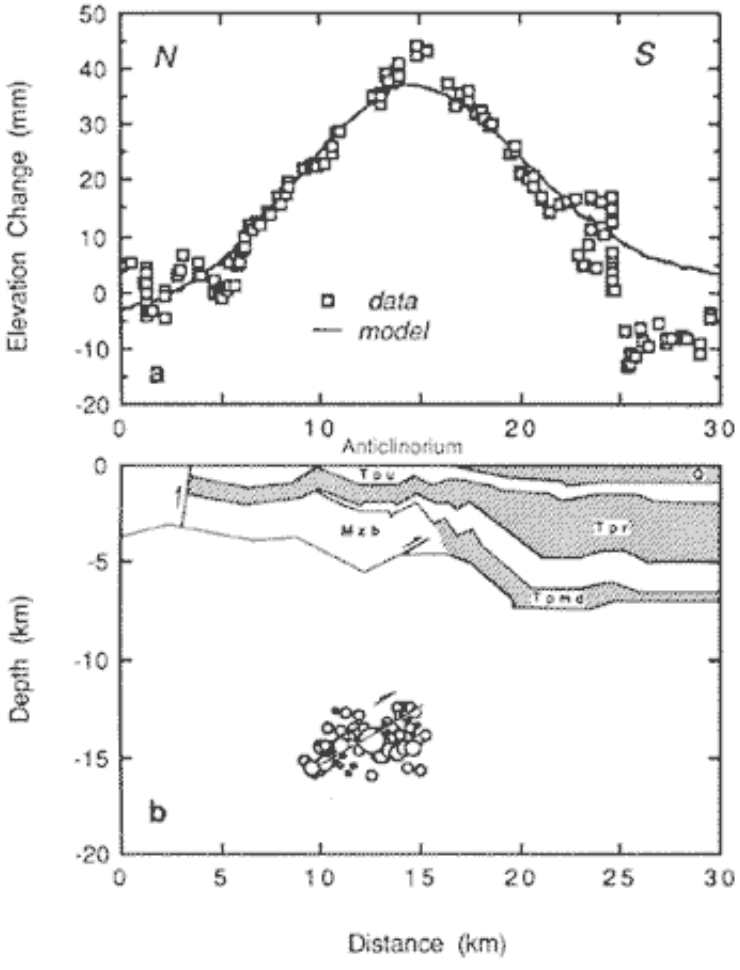

Fig. 2. (a) Profile of observed coseismic elevation changes for line 1, projected on a N-S azimuth, together with predicted changes (line)

ANALYSIS

Coseismic Model

We seek the simplest dislocation plane that can explain the observed elevation changes and passes through the hypocenter of the main shock. Fault slip is approximated by uniform displacement on a rectangular surface embedded in an elastic half-space, using the expressions of Mansinha and Smylie [1971]. As long as the contrast in elastic modulii between the Los Angeles basin sediments and the underlying rocks is modest (less than a factor of 2), we can neglect the increase in stiffness with depth. The coseismic elevation changes and their associated uncertainties are plotted in Figure 7 for line 1 (top right) and line 2 (bottom right) with uncertainties indicated by error bars. The observation weights are inversely proportional to their uncertainties. The network rms signal-to-noise ratio measures the size of the coseismic deformation relative to its uncertainty and thus represents the quality of the observations. The rms signal strength is the mean elevation change for a typical observation, and the pure error is the uncertainty associated with that observation. For a network of observations, the rms misfit of model to data is

azimuth, together with predicted changes (line) for the coseismic model. (b) Schematic geological cross section of the uppermost 5 km in northern Los Angeles basin showing Santa Monica Mountains anticlinorium [from Davis et al., [this issue], aftershocks magnitude proportional to size of circles (see Figure 1a). Geologic units: M2b, undifferentiated schist; Tpmd, uppermost Miocene and lowermost Pliocene (Delmontian); Tpr, Pliocene (Repetto fm.); Tpu, upper Pliocene; Q, Quaternary.

$$\left[\frac{1}{N-K}\sum_{i=1}^{N} r_i^2\, w_i^2\right]^{1/2} \quad (1)$$

where $r_i = o_i - c_i$ is the difference between observed and predicted elevation of the ith observation. To calculate the rms signal strength, c_i is the constant baseline given by inversion. N is the number of observations (214) , and K is the number of free parameters (typically 6 in this study). The inversion weight w_i is defined by

$$w_i = \frac{\overline{\sigma}}{\sigma_i} \quad (2)$$

where σ_i^2 is the uncertainty of the ith observation and

$$\overline{\sigma}^2 = N\left[\sum_{i=1}^{N} \sigma_i^{-2}\right]^{-1} \quad (3)$$

The rms pure error for the network is defined by

$$\left[\frac{1}{N}\sum_{i=1}^{N}\sigma_i^2\right]^{1/2} \quad (4)$$

Here the rms signal strength is 24.6 mm and the rms pure error is 4.8 mm, giving a signal-to-noise ratio of 5.1 (Figure 7). More details of the statistical measures are given by Barrientos et al. [1987, Printable arcticle 1.75Mb].

Model Fit

The geometry of a fault plane is characterized by its dimensions along strike (length), down-dip direction (width), and dip. To specify uniquely the location of a fault plane, one also needs to know the strike and the spatial coordinates of one corner of the fault plane. The slip magnitude is a free parameter to be solved by inversion. Because a constant can be freely added to all values of the elevation change, we lack an absolute reference frame for the elevation changes. Thus we also solve for the elevation change of the BM at the

junction of the two lines as a free parameter (the junction is indicated by a cross in the profiles).

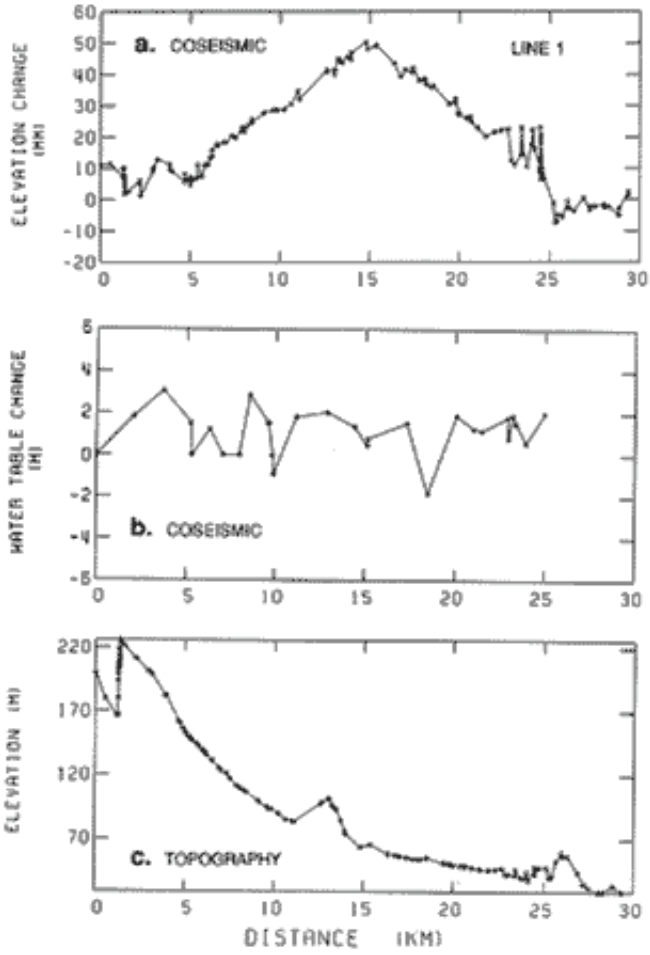

Fig. 3. (a) Profile of 1987-1986 coseismic elevation changes along line 1, projected on a N-S azimuth. (b) Profile of 1987-86 water table changes in water wells close to leveling line 1. (c) Leveling route topography.

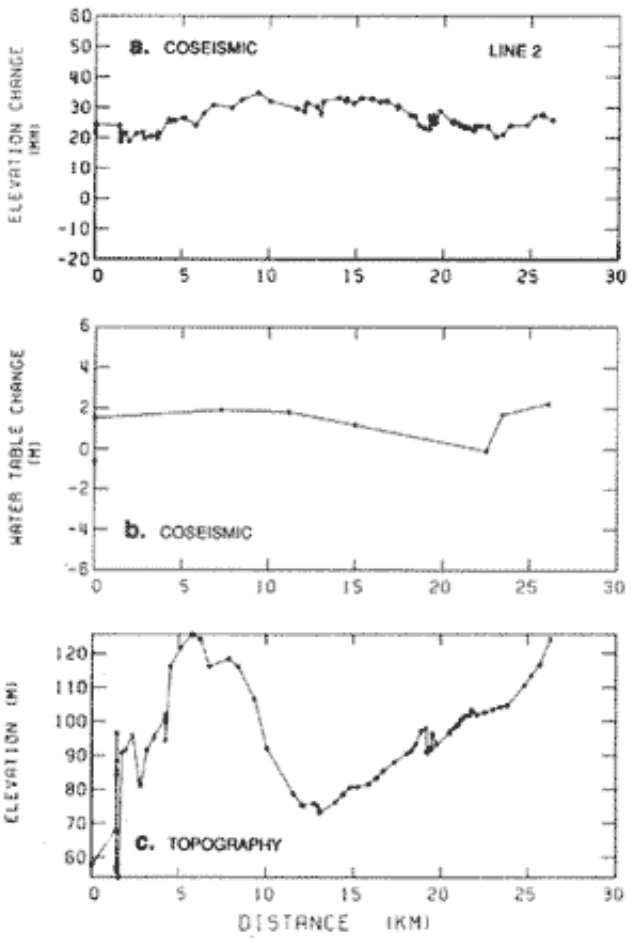

Fig. 4. (a) Profile of 1987-86 coseismic elevation changes along line 2, projected on a E-W azimuth. (b) Profile of 1987-1986 water table changes in water wells close to leveling line 2. (c) Route topography.

Several of the fault parameters can not be determined unambiguously from the leveling data. The vertical deformation caused by an earthquake is insensitive to small amounts of strike-slip motion. Since the focal mechanism of the Whittier Narrows main shock is dominantly thrust motion [Hauksson et al. 1988], we constrain the slip on the fault plane to be pure dip slip. Due to the symmetry in the seismic radiation pattern, either the gently north dipping or the steeply south dipping nodal planes are consistent with the main shock focal mechanism. However, we find that if the steeply south dipping fault is located so that the predicted deformation best matches the observations, the fault plane does not pass within 2 km of the main shock hypocenter. On the basis, we eliminate the steeply south dipping plane from further consideration and instead concentrate on the gently north dipping plane. Such a gently north dipping plane also has the attribute that it passes through most of the initial aftershocks, although neither of these criteria guarantees that we have chosen the correct plane. The vertical deformation is insensitive to the strike of the fault plane, because the predicted deformation pattern is a nearly radially symmetric dome (Figure 8a). Since changes of

strike of +-30° can not be reliably distinguished, we consider only a fault strike of N90°E, as suggested by main shock focal mechanism [Hauksson et al. 1988]

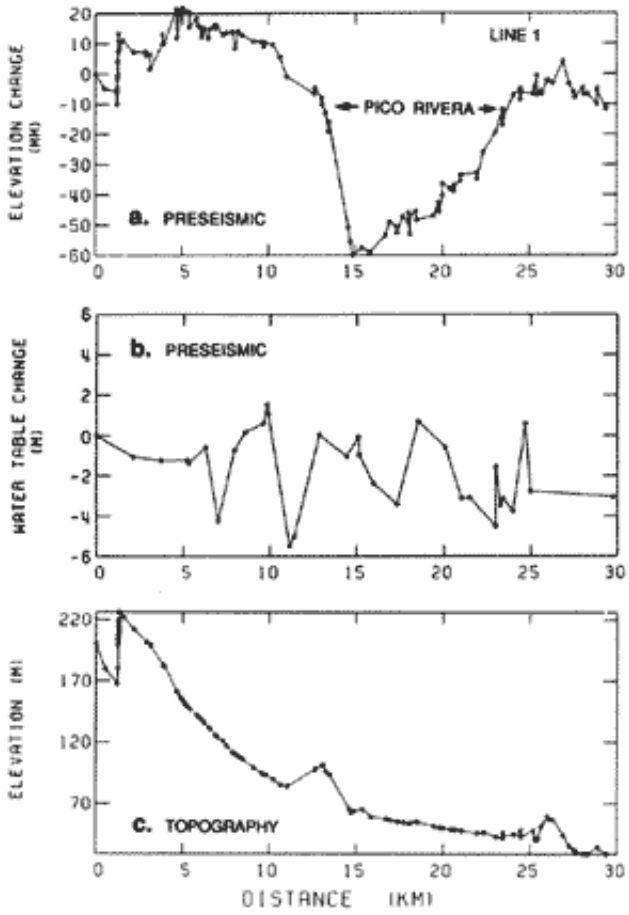

Fig. 5. (a) Profile of 1986-75 preseismic elevation changes along Line 1, projected on a N-S azimuth. (b) Profile of 1986-1975 water table changes in water wells close to leveling line I. (c) Route topography.

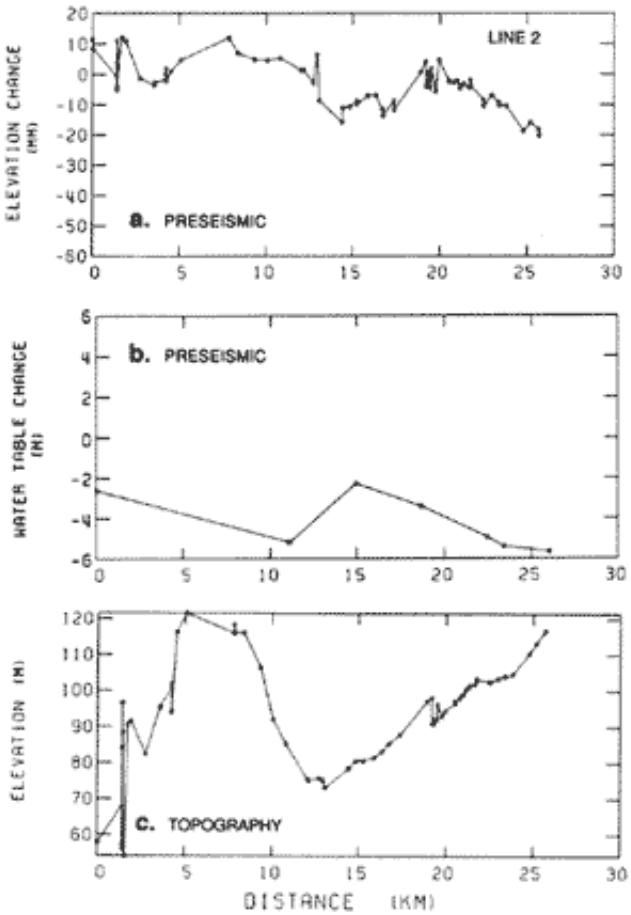

Fig. 6. (a) Profile of 1986-1975 preseismic elevation changes along line 2, projected on a E-W azimuth. (b) Profile of 1986-1975 water table changes in water wells close to leveling line 2. (c) Route topography.

Because the source depth of the Whittier Narrows main shock is 1-2 times greater than either the fault dimension (length or width), the model fault depth trades off with fault area. In other words, a deeper, smaller fault with greater slip can produce surface deformation similar to a shallower, larger fault with smaller slip. This trade-off makes it difficult to resolve both the depth and area of the fault plane. The moment M_o released during the earthquake

$$M_o = \mu \sum u\, A$$

is proportional to the product of the slip (u) and the area (A). The moment can be increased by a factor of 4 for a deeper and larger earthquake with larger fault area. Thus only the lower limit of the moment is better

constrained than the fault dimensions or slip.

We chose the following six variables as free parameters in developing the dislocation model: fault length, width, dip, depth of burial, latitude and longitude (x and y coordinates of the east end of the upper fault edge). A systematic search of the parameter space was carried out to find the best fit, in which the slip and baseline level (zero datum) were solved by leastsquares inversion. Uncertainties in inversions are also calculated. Forward modeling is carried out by exploring all permutations of the 6 free parameters over a given range and increment, requiring 12,000 runs.

We find three dislocations models (A, B, and C) which best fit the observations on vertical deformation in the Whittier Narrows area:

Model A: *Minimum moment*. This represents the smallest fault surface which can explain the geodetic observations; the fault plane coincides roughly with the aftershock zone. Tests reveal that when the assumed fault area is slightly greater or smaller than that given by model A, the fit deteriorates. Here fault length along strike is 4.5 km, down-dip width is 6 kill, the depth of the upper end of the fault plane is 12 km, the dip angle is 30°, the coseismic slip is 1.10 m, the static stress drop, delta sigma, is 17.5+-5.0 MPa (175+-50 bar), and the geodetic moment, M_o=0.96 x 10^{25} dyne cm (Figure 7 and; Table 2). The rms misfit-to-noise ratio is 0.93, which indicates that the model residuals are about the size of the noise. The surface projection of the fault plane is displayed on the left side of Figure 7, together with the distribution of bench marks used in the leveling. The comparisons of the predicted and observed coseismic elevation changes are shown on the right side of Figure 7 for line 1 and line 2. Visual inspection suggests that along line 1 the predicted deformation matches the coseismic elevation changes well except at the southern end, where uncorrected Santa Fe Springs oil field deformation (shown in Figure 1b) may be substantial. Although the overall fit of prediction to observation is also satisfactory in line 2, the model systematically underestimates the deformation on the eastern most 8 km by 1-2 standard deviations (7 mm).

The best fit fault parameters of model A, as well as the range tested, are listed in Table 2. The quoted uncertainties in Table 2 represent a 5% increase in the sum-squared residuals, with all other parameters free to change and thus reflects the covariances in the free parameters. Contours of predicted vertical displacements are shown in Figure 8a and the predicted horizontal motion is shown in Figure 8b. Since the predicted horizontal vectors nowhere exceed 14 mm, and changes in baseline length (the difference of any two vectors) never exceed 20 mm, the existing electronic distance or space geodetic measurements in the area are not precise enough to warrant resurvey.

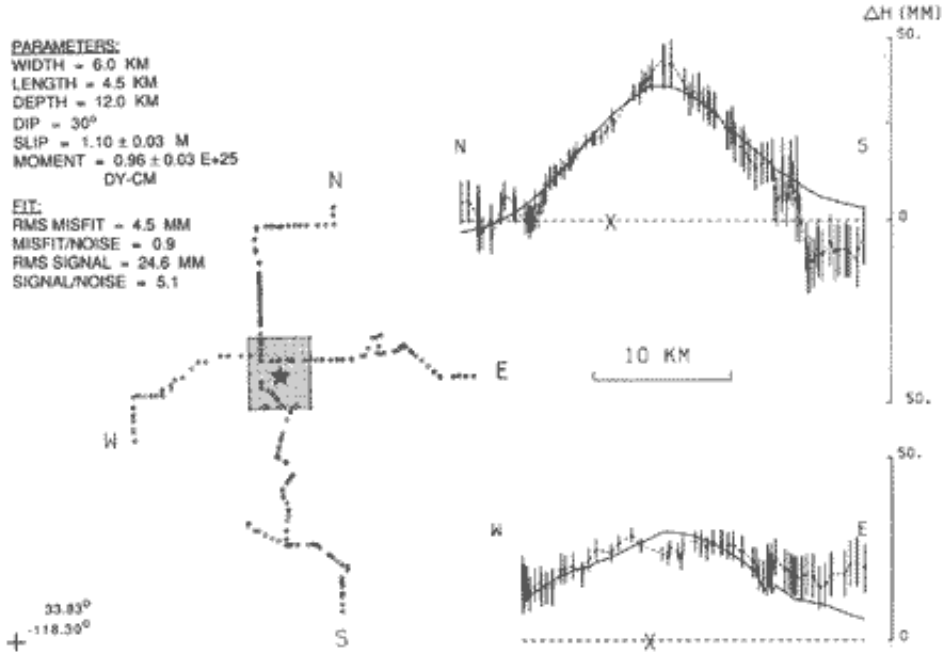

Fig. 7. Best single-plane model (model A) for Whittier Narrows earthquake, which yields lower limit of the geodetic moment. The left map shows the data distribution and the surface projection of the fault plane. The observations (dashed line with vertical error bars) and predicted coseismic elevation changes (solid line) along the N-S line are shown at top right. The observed and predicted elevation changes along the W-E line are shown at the bottom right.

Model B: *Maximum moment*. If we no longer require the fault plane to be in the vicinity of the aftershock zone, there are two additional solutions (model B and model C in Figure 9) which correspond to local minima in the misfit function. Model B represents a fault plane elongated in the direction of the fault strike (Figure 9 and Table 3). Here fault length along strike is 12 km, down-dip width is 4 km, the depth of the upper end of the fault plane is 12 km the dip angle is 34°, the coseismic slip is 0.71 m, and the geodetic moment is 1.09×10^{25} dyne cm. The rms misfit-to-noise ratio for model B is 0.83.

Models A and B give geodetic moments that differ only by 10%. Most of the improvement of model B over model A comes from the fit to the deformation at the east end of line 2. Model B represents a fault plane extending 4 km eastward of model A. No aftershocks were detected in this eastern region, leaving its significance dubious.

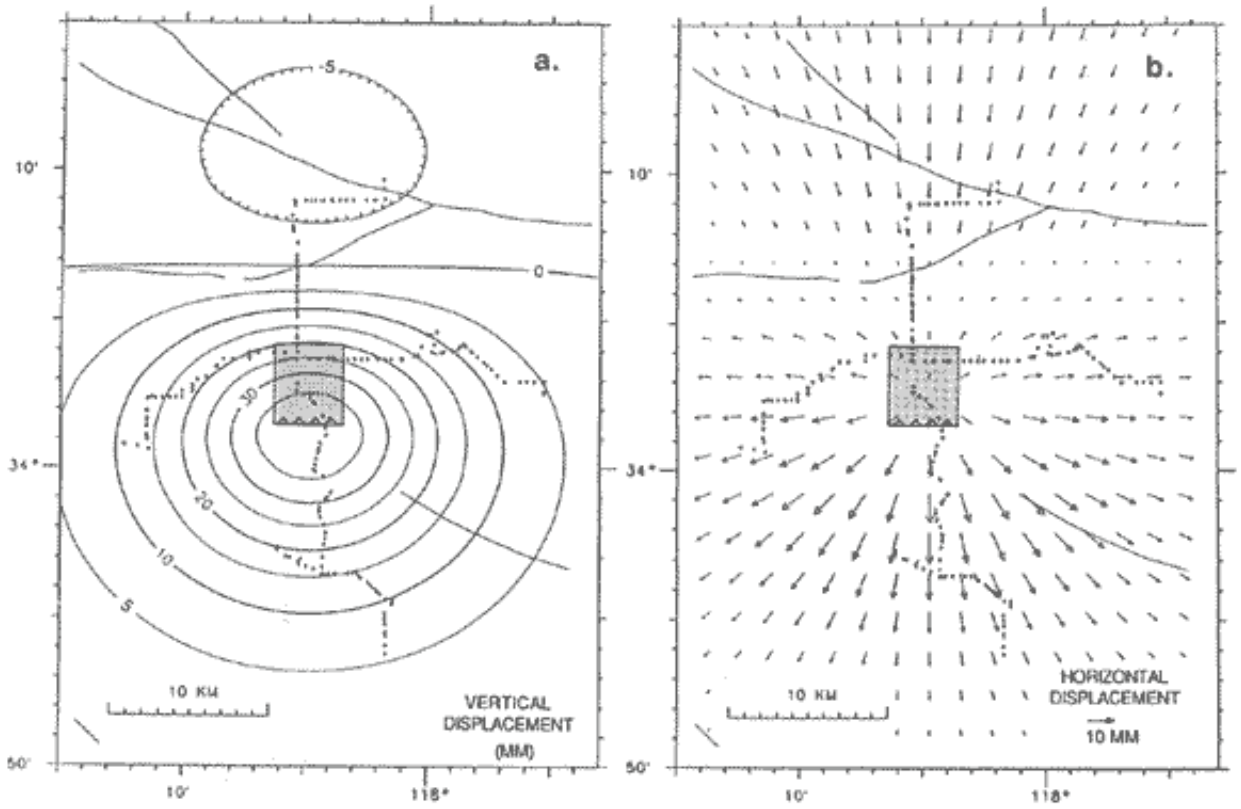

Fig. 8. Predicted (a) vertical and horizontal (b) displacements for model A. Displacements for Model B are not significantly different from those shown here.

Following the suggestion of Linde and Johnston [this issue], we found another solution with much steeper fault plane and larger fault area. Here fault length along strike is 5.9 km, down-dip width is 25.6 km, and the depth of the upper end of the fault plane is 13.2 km. The fault plane strikes N62W, dips 50°; the coseismic slip is 0.86 m with a rake of 124°. The rms misfit-to-noise ratio is 0.90. The inferred geodetic moment is 3.75 x 10^{25} dyne cm, significantly greater than that of model A. This solution requires much larger absolute elevation changes; in other words a greater shift in the baseline is required. Since we lack an absolute reference frame for the elevation changes, we can not exclude this model. However, we note that this model fault plane does not pass through the main shock hypocenter or the aftershock zone and thus regard it as an unlikely candidate. Such a model could be tested, however, by extending one or more of the leveling lines outside of the coseismical1y deformed region.

DISCUSSION

DISCUSSION

Concordance of Geodetic and Seismic Estimates of the Earthquake

Our best measure of the earthquake is the lower bound on the of the long-period (10^{-8} Hz) geodetic moment, 1.0+- 0.2 x 10^{25} dyne-cm, corresponding to a moment-magnitude, M = 6.0. Recorded teleseismic amplitudes (10^{-1} Hz) correspond to a seismic moment of 0.86 x 10^{25} dyne cm [Dziewonski et al., 1988]; short-and long-period body waveform data correspond to a moment of 1.4 x 10^{25} dyne cm [Bent and Helmberger, this issue]; regional broadband recordings yield a moment of 1.0+-0.06 x 10^{25} dyne-cm [Bolt et al., this issue]. Agreement between seismic moment and lower limit of static moment suggests that this earthquake released most of its moment at seismic frequencies.

The location of the Whittier Narrows fault plane is accurately controlled by the geodetic data, since, for a planar fault, the upper edge of the fault must lie beneath the position of peak uplift. In model A, the main shock is located in the center of the rupture plane (Figure 7) and the fault area lies completely within the 3-day ring of aftershocks (see Figure la). In model B, the main shock also lies near the center of the fault plane. This suggests that the Whittier Narrows earthquake nucleated near the center of fault plane and propagated radially outward.

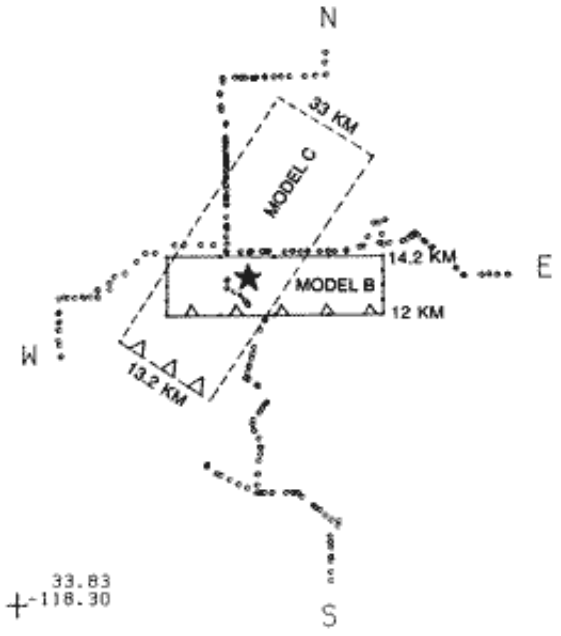

Fig. 9. Alternative solutions for Whit tier Narrows coseismic deformation, which yield larger moments. The depths of the upper and lower edges of the fault planes are shown adjacent to the surface projection of the fault. Model B corresponds to a geodetic moment of 1.09 x 1025 dyne cm. Model C has a moment of 3.75 x 1025 dyne cm resulting from the larger and deeper fault plane.

Unlike the Whittier Narrows earthquake, the May 2, 1983, Coalinga, California, shock reveals substantial non seismic slip. The Coalinga rupture nucleated at the upper edge of the fault and propagated down-dip. The amplitude of the Coalinga fold increased by nearly 20% during the 4 years since the earthquake. The continued folding can be explained by 0.5 m of postseismic slip on the fault plane [Stein and feats 1989]. Such postseismic deformation at Whittier Narrows is beneath the limits of resolution by repeated leveling surveys but has not been detected by a borehole dilatometer network [Linde and Johnston, this issue].

Consistent with the seismological estimate, our dislocation models indicate that the fault plane at Whittier Narrows lies at a depth of 12-17 km, which is deeper than most Los Angeles basin earthquakes. For example, southwest of Whittier Narrows earthquakes along the Newport-Inglewood fault zone show a depth distribution of 6-11 km, which is similar to average seismogenic depths elsewhere in southern California [Hauksson, 1987]. The unusually deep fault plane at the Whittier Narrows area might suggest a loc 1 depression of the brittle-ductile transition zone, which could be caused by low heat flow [Mayer. 1987].

TABLE 2. Parameters of Whittier Narrows Earthquake From Leveling

Measurements: Model A

Fixed Parameter				Value	
Strike				N90.0° E	
Rake				90.0°	
Free Parameter	Tested Range Min	Max	Increment	Best Fit	Uncertainty (95% residual)
Length (along strike)	2.0	8.0	1.0	4.5 km	1.0
Width (down dip)	3.0	9.0	1.0	6.0 km	1.0
Depth (to fault top)	9.0	15.0	1.0	12.0 km	1.0
Dip angle	25°	34°	2°	30° N	2°
Latitude*	33.59°	34.07°	0.04°	34.03° N	0.05°
Longitude*	118.03°	118.07°	0.02°	118.05° W	0.02°
Inverted Parameter	[misfit/noise = 0.9]			Value	Uncertainty
slip, m				1.09	0.30
Moment, dyne-cm				0.96×10^{25}	0.20×10^{25}

* East end of fault's upper edge.

TABLE 3. Parameters of Whittier Narrows Earthquake From Leveling Measurements: Model B

Fixed Parameter				Value	
Strike				N90.0° E	
Rake				90.0°	
Free Parameter	Tested Range Min	Max	Increment	Best Fit	Uncertainty (95% residual)
Length (along strike)	42.0	14.0	2.0	12.0 km	2.0
Width (down dip)	3.0	8.0	1.0	4.0 km	1.0
Depth (to fault top)	9.0	15.0	1.0	12.0 km	2.0
Dip angle	28°	38°	2°	34° N	2°
Latitude*	33.59°	34.07°	0.04°	34.03° N	0.05°
Longitude*	117.59°	118.08°	0.04°	118.00° W	0.05°
Inverted Parameter	[misfit/noise = 0.8]			Value	Uncertainty

slip, m	0.71	0.30
Moment, dyne-cm	1.09×10^{25}	0.20×10^{25}

* East end of fault's upper edge.

Coseismic Growth of the Santa Monica Mountains Anticlinorium

The Whittier Narrows earthquake provides unambiguous evidence for the coseismic growth of folds, as slip at depth caused the Santa Monica Mountains anticlinorium to uplift 50 mm. Although slow deformation must also occur between earthquakes, the close association between coseismic deformation and the Quaternary geologic structure is unlikely to be coincidental (Figure 2). There is a correlation between the historical seismicity and both faults and folds with a band of small-to-moderate earthquakes lying within 5 km of the Santa Monica Mountains anticlinorium identified by Davis et al. [this issue] (Figure 10). The 1987 event occurred at the eastern end of Elysian Park anticline, an individual element within the Santa Monica Mountains anticlinorium.

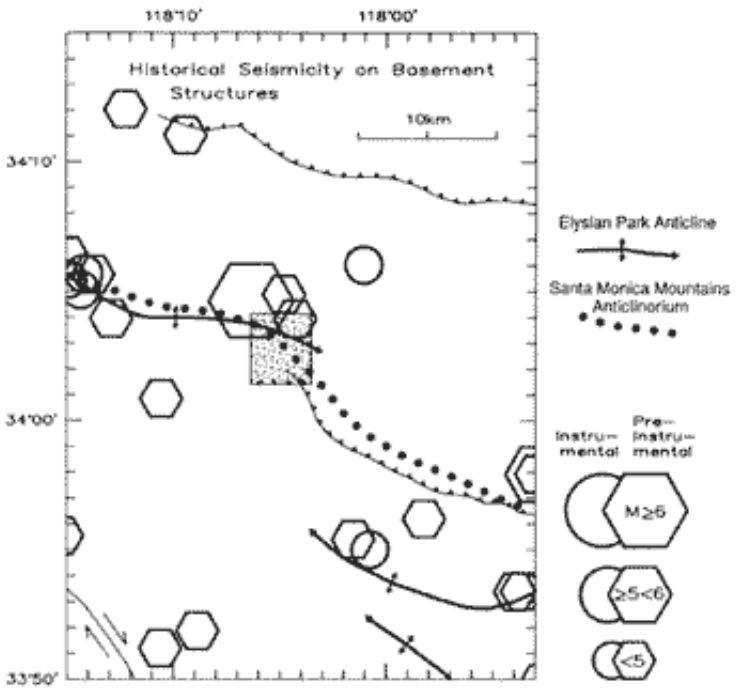

Fig. 10. Historical earthquakes from 1800 with Modified Mercalli intensities MM>VII, and instrumental earthquakes with ML>3 from 1970 to 1988 (modified from Yerkes [1985]). The fault plane of model A is stippled. The largest earthquake occurred in 1855, MMVIII (equivalent to M=6). The Santa Monica Mountains anticlinorium was identified by Davis et al., (this issue). Note that much of the seismicity locates near anticlines rather than surface faults.

Geomorphic evidence for late Quaternary uplift of Santa Monica Mountains anticlinorium can be seen in topographic maps surveyed in 1893-1994 at a contour interval of 25 feet (7.6 m) [U.S. Geological Survey, 1896,1897,1900, 1901]. These show the surface morphology prior to urban development and man-made channeling of stream (Figure 11). An abandoned water gap (Coyote Pass; dotted in Figure 11) through the Santa Monica Mountains anticlinorium appears to be the path of the ancestral Rio Hondo, which is now deflected around the eastern nose of the Montebello Hills. Because the former stream path now rises one contour interval from an originally sloping gradient, there has been at least 25 feet (8 m) of uplift since abandonment. Based on the approximate 0.23 Ma age for the alluvial surface [Crook et al., 1987], we estimate an uplift rate for the anticline of >0.03 mm/yr. Accelerator ^{14}C dating of detrital charcoal in the gap would provide a constraint on the rate of anticlinal uplift at this site; although the channel has been regraded for Monterey Pass Road. The San Gabriel River and Rio Hondo converge within 1.5 km of each other in the Narrows and maintain slightly divergent courses for the remaining 30 km to the Pacific Ocean (Figure II). This may indicate that uplift of the antiform has narrowed what was once a broader topographic gap, a further indication of Quaternary uplift.

Earthquake Recurrence and Implications for Earthquake Forecasts

An earthquake repeat time for the Whittier Narrows site can be estimated from geodetic observations, geological structure, and historical seismicity. The simplest approach is to relate the long-term anticlinal uplift rate to the coseismic uplift. Assuming that the rate of tectonic activity has been constant since the inception of the Santa Monica Mountains anticlinorium at 3 Ma, we obtain an uplift rate of 0.5 mm/yr based on the observed 1.5 km structural relief of the anticline. This is less than the growth rates of several folds along the eastern margin of the California coast ranges [Stein and King, 1984; Zepeda and Keller, 1986]. We further assume that the seismicity in the Whittier Narrows area is characterized by earthquakes that permanently uplift the ground 50 mm (e.g., M <6), which is consistent with the 125-year historical record which shows no earthquakes larger than M=6. We then obtain an earthquake repeat time of about 100 years. This is equivalent to a moment release rate of 1×10^{23} dyne cm/yr.

Such an estimate suffers from the fact that slip on adjacent patches of the presumed thrust fault would also contribute to uplift at Whittier Narrows. A model of uplift caused by one meter of slip on a laterally continuous fault with the same depth, dip, and down dip width as the Whittier Narrows event produces about 130 mm of uplift (rather than 50 mm for a fault only 5 km along strike), about one third of which is recovered interseismically by postearthquake relaxation [see King et al., 1988]. Thus the uplift expected for 1 m of slip on the blind thrust is approximately l00 mm, yielding a repeat time of 200 yr and a rate of moment release of 5×10^{22} dyne cm/yr.

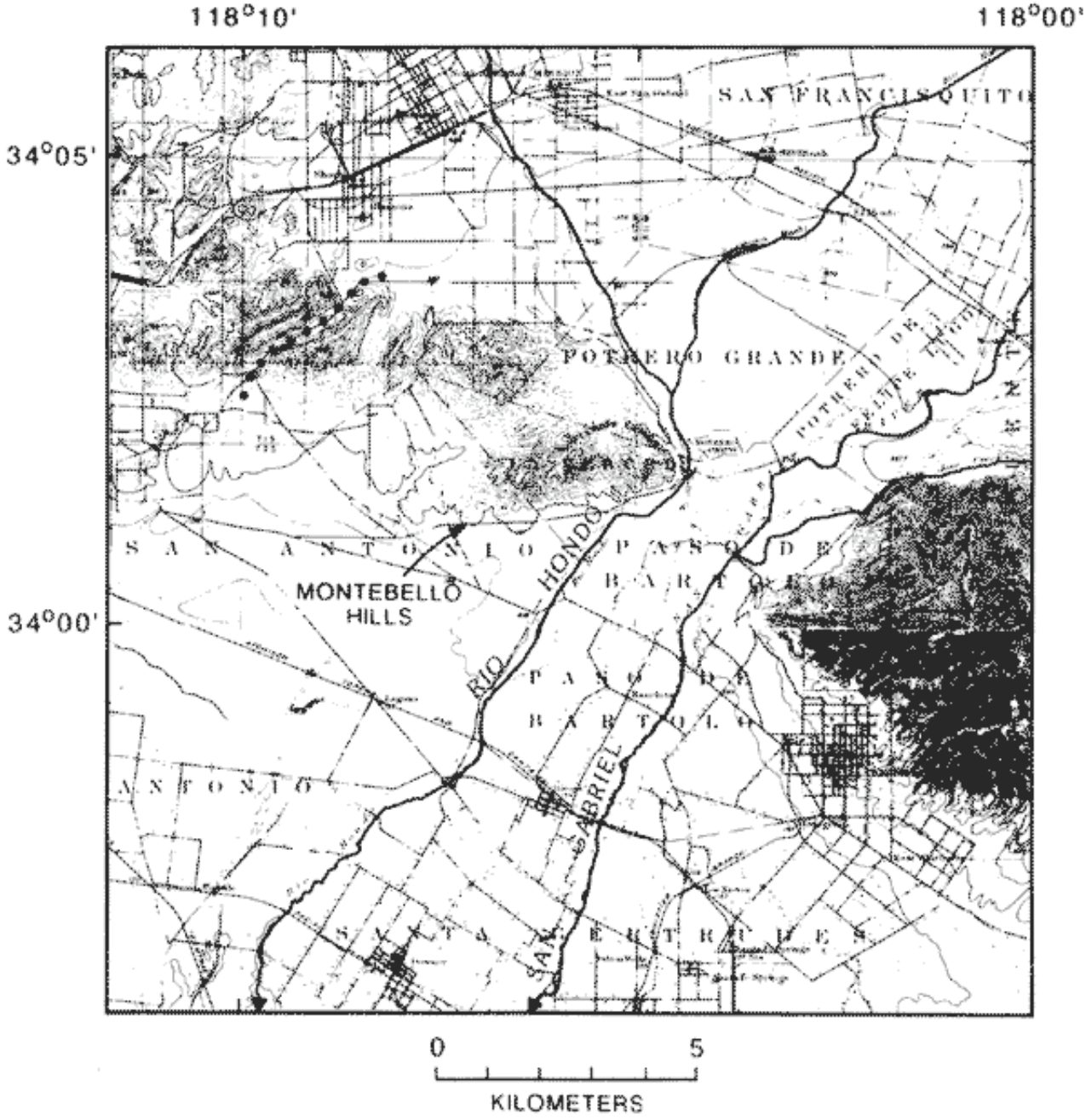

Fig. 11. Topographic map surveyed in 1893-1994 [U.S. Geological Survey, 1896; 1900] at a contour interval of 25 feet, revealing the surface morphology prior to urban development and stream channelization. Probable path of ancestral Rio Hondo River dotted; grade now uplifted one contour interval (~25 feet).

We can make a nearly independent estimate of the earthquake repeat time from a comparison of the geological horizontal contraction rate and the horizontal component of the coseismic slip. Using a retrodeformable cross section constructed from oil well data, Davis et al., [this issue] estimated a long-term horizontal contraction rate of 11 mm/yr across the Los Angeles basin, perhaps half of which occurs as slip on the blind thrust beneath the Santa Monica Mountains anticlinorium. If coseismic slip of 0.7-1.0 m is characteristic of earthquakes in the Whittier Narrows area (M <6), we find an earthquake repeat time of

140-200 years. If several faults, such as the belt of folds just north of Palos Verdes Peninsula (PV in Figure 12), accommodate the shortening, then the repeat times would lengthen by a commensurate amount.

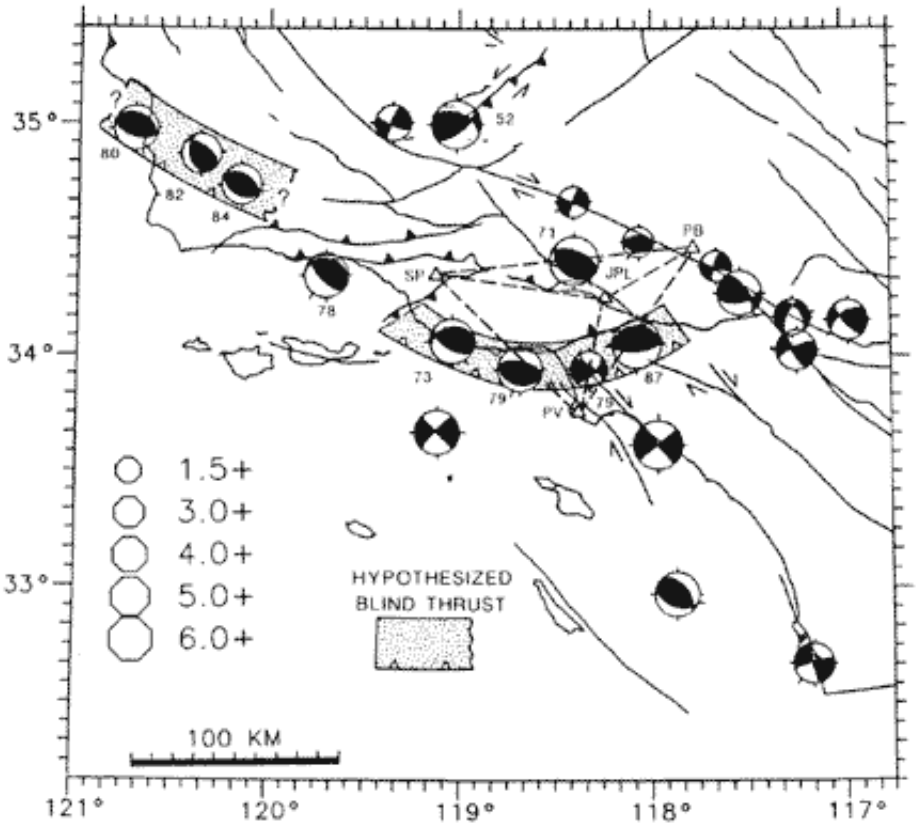

Fig. 12. Map of active faults in southern California, with focal plane solutions for well-recorded earthquakes [from Hut ton et al., 1988]. Hypothesized blind thrust sheets are stippled; very long baseline interferometry network is dashed.

The Santa Monica Mountain anticlinorium spans 75 km along the northern margin of the Los Angeles basin [Davis et al., this issue], and may extend offshore into Santa Monica Bay for another 70 km. Hauksson and Saldivar [1986] and Hauksson et al. [1988] show that the structure is the site of several moderate earthquakes during the past 15 years (Figure 12). Hutton et al. [1988] have identified a remarkable 300-km-long alignment of thrust events from Point Sal (35°N/120.8°W); event marked by year of occurrence, "80," in Figure 12) to the Whittier Narrows event ("87" in Figure 12). We suggest here that these events have occurred on an underlying blind thrust fault, which is truncated or segmented by the active south dipping Oak Ridge reverse fault (6-12 mm/yr slip rate [see Yeats, 1988]). Thus we consider here only the possibility of a 150-km-long thrust beneath the Los Angeles basin, and a separate 100-km-long thrust near Point Sal. It is intriguing that earthquakes have migrated to the east on both proposed thrusts (Figure 12), although this could be coincidental.

The dislocation modeling indicates that the segment which ruptured during the Whittier Narrows earthquake was 3.5-14.0 km long (at the 95% level of confidence). If a blind thrust lies beneath the 150-km-long antiform, as shown schematically in Figure 12, we would expect at least six and as many as 35 rupture patches along the E- W trending thrust. If each patch has a characteristic earthquake repeat time of 200 years, an earthquake would occur somewhere along this 150-km-longthrust every 5-18 years. Instead, the 125-year historical record complete to M>5.5 [Yerkes, 1985] reveals only one event per 25 years, indicating a deficit in moment release.

Apart from any inaccurate assumptions as to the length of the thrust and its contemporary slip rate, there are two viable explanations for the moment deficit, fault creep or infrequent large earthquakes:

Fault creep. The blind thrust fault could have a substantial component of creep. Sykes and Quittmeyer [1981] found that underthrust zones at subduction plate boundaries exhibit a range of behavior, from purely

seismic to aseismic, with a typical seismic slip to total slip ratio of 62%. Engeln et al. [1986] also found that nearly all Mid-Atlantic Transform faults exhibit some aseismic slip. Because part of the hypothesized thrust lies at depths >15 km, crustal material might exhibit partially ductile behavior. Mayer's [1987] estimate of the geothermal gradient of >27°C/km in the upper 6 km yields an extrapolated temperature of about 400°C at 15 km. At these pressure and temperature conditions, quartz shows significant amount of ductility due to solid state creep [cf. Kirby, 1983].

Infrequent larger earthquakes. The alternate explanation is that larger earthquakes occur beneath the Los Angeles basin, with periodicity much greater than 100 years. An example of such an event in a similar tectonic environment is the 1952 M=7.2 Kern County, California, earthquake (event "52" in Figure 12). The western half of the White Wolf fault, on which the Kern County earthquake occurred, is buried 5 km beneath the ground surface [Stein and Thatcher, 1981], and partly underlies an active Quaternary fold, Wheeler Ridge anticline. On the basis of the Quaternary slip rate and the coseismic slip, Stein and Thatcher [1981] suggested that the probable repeat time for this earthquake is 1000 year. If such events also characterized the Los Angeles basin 120 km to the south, the absence of large earthquakes during the 125-year historical record would not be surprising.

CONCLUSIONS

We observe 50 mm of coseismic anticlinal uplift suggesting that, at least in part, the Santa Monica Mountains anticlinorium grows by episodic earthquake uplift, rather than by progressive deformation. This inference is consistent with other recent thrust events beneath active anticlines, which together provide pervasive evidence that folds grow dominantly by earthquake deformation.

A geodetic model of coseismic deformation suggests a surprisingly deep, gently north dipping thrust fault beneath the Los Angeles basin, which had not been previously recognized or evaluated for its earthquake potential. We find a lower limit of the geodetic moment of $1.0+-0.2 \times 10^{25}$ dyne cm; the deduced coseismic slip ranges over 0.7-1.1 m. The fault rupture plane ranges over 3 x 5 to 6 x 10 km. The upper edge of the slip surface lies directly beneath Whittier Narrows. It is likely that the fault patch that ruptured during the Whittier Narrows earthquake is only one segment of a larger thrust fault, which has sustained similar small to moderate earthquakes during the last 125 years.

Given a Quaternary slip rate of 11 mm/yr on a 150-km-long blind thrust, or uplift rate of 0.5 mm/yr on the fold, a moment release rate of 1×10^{23} dyne cm/yr at Whittier Narrows, or $1\text{-}4 \times 10^{24}$ dyne cm/yr over the entire thrust is expected. This yields a M=6 earthquake in the northern Los Angeles basin roughly every 10 years, several times greater than that inferred from historical record. Unless Davis et al's [this issue] age or amplitude of the Santa Monica Mountains anticlinorium is in error, this deficit in moment release rate implies that either aseismic slip dominates beneath the Los Angeles basin or that the thrust ruptures during infrequent larger earthquakes, with repeat times greater than the 125 year historical record.

Further geodetic measurements are needed to resolve the moment deficit paradox in the Los Angeles basin. First, measurement of the rate of N-S contraction from the San Gabriel mountains to the Palos Verdes Peninsula, using existing (1980-88) Very Long Baseline Interferometry observations or more recent Global Positioning System observations (1987-1988) is required. Stations at Jet Propulsion Laboratory (JPL) at the foot of the San Gabriel mountains, Pearblossom, just north of the San Andreas fault, and Santa Paula, in the western Transverse Ranges are well suited to this task (Figure 12). These stations possess good (but not simultaneous) VLBI measurements since 1982. The geodetic measurements are necessary to provide an

independent test of the geologically inferred 11 mm/yr N-S contraction rate. The second task is to examine the 90-year-old historical leveling observations across the active anticlines carried out by the City and County of Los Angeles, the U. S. Geological Survey and the National Geodetic Survey, to find if there is evidence for aseismic anticlinal growth. Lamar and Lamar [1973] performed a limited analysis of leveling surveys, but they used adjusted data, which are inappropriate for the purpose of detecting small motions, as the secular uplift rate may be as low as 0.5 mm/yr. Nontectonic subsidence poses a severe problem to the unambiguous identification of anticlinal uplift, but the effort would be nevertheless useful to falsify the hypothesis that all uplift is coseismic.

Read the APPENDIX

REFERENCES

Barrientos, S.E., R.S. Stein, and S.N. Ward. Comparison of the 1959 Hebgen Lake, Montana and the 1983 Borah Peak, Idaho, earthquakes from geodetic observations, *Bull. Seismol. Soc. Am.*. 77, 784-808. 1987. [Printable arcticle 1.75Mb]

Bent, A.L., and D.V. Helmberger, Source complexity of the October 1, 1987, Whittier Narrows earthquake, *J. Geophys.* Res., this issue.

Bolt, B.A., A. Lomax, and R.A. Uhrhammer. Analysis of regional broadband recordings of the 1987 Whittier Narrows, California earthquake, *J. Geophys.* Res., this issue.

Conservation Committee of California Oil Producers, Annual review of California oil and gas production, 1974-1987.

Crook, R., C.R. Allen, B. Kamb, C.M. Payne, and R.J. Proctor, Quaternary geology and seismic hazard of the Sierra Madre and associated faults, western San Gabriel Mountains, Recent Reverse Faulting in the Transverse Ranges, California, *U.S. Geol. Surv. Prof Pap.*, 1339,27-64, 1987.

Davis, T.L., J. Namson, and R.F. Yerkes, A cross section of Los Angeles basin: Seismically active fold and thrust belt, the Whittier Narrows earthquake and earthquake hazard along the northern edge of the Los Angeles basin, *J. Geophys.* Res., this issue.

Dziewonski, A.M., G. Ekstrom, J.H. Woodhouse, and G. Zwart, Centroid-moment tensor solutions for October-December, 1987, Phys.Earth Planet. Inter, in press, 1988.

Ekstrom, G. A., A broad band method of earthquake analysis, Ph.D. thesis, Harvard Univ., Cambridge, Mass., 216 pp., 1987.

Engeln, J. F., D.A. Wiens, and S. Stein, Mechanisms and depths of Atlantic transform fault earthquakes, *J. Geophys.* Res., 91, 548-578, 1986.

Federal Geodetic Control Committee, Standards and specifications for geodetic control networks, Nat. Geod. Surv., Rockville, Md., 1984.

Hauksson, E., Seismotectonics of the Newport-Inglewood fault zone in the Los Angeles Basin, southern California, *Bull. Seismol. Soc.Am.*, 77,539-561, 1987.

Hauksson, E., and G.V. Saldivar, The 1930 Santa Monica and the 1979 Malibu, California, earthquakes, *Bull. Seismol. Soc. Am.*, 76, 1542-1559,1986.

Hauksson, E., et al., The 1987 Whit tier Narrows earthquake in the Los Angeles metropolitan area, California, *Science*, 239, 1409-1412, 1988.

Hutton, K.L., L.M. Jones, E. Hauksson, and D.D. Given, Seismotectonics of southern California, in *Neotectonics of North America, Decade N. Am. Geol.*, vol., edited by D.B. Slemmons, E.R. Engdahl, D. Blackwell, and D. Schwartz, Geological Society of America, Boulder, Colo., CSMV-1, 1989.

Jackson, D.D., W .B. Lee, and C. Liu, Height dependent errors in southern California leveling, in *Earthquake Prediction: An International Review*, Maurice Ewing Ser. vol 4, edited by D.W. Simpson and P. G. Richards, pp. 457-472, AGU, Washington D.C., 1981.

King, G.C.P., R.S. Stein, and J.B. Rundle, The growth of geological structures by repeated earthquakes; 1, Conceptual framework, *J . Geophys. Res.*, 93, 13,307-13,318, 1988.

Kirby, S.H., Rheology of the lithosphere, *Rev. Geophys.* 21, 1458-1487, 1983.

Lamar, D.L., and J.V. Lamar, Elevation changes in the Whittier fault area, Los Angeles Basin, California, in edited by D.E. Moran et aI., *Geology, Seismicity, and Environmental Impact*, Association of Engineering Geologists, Palo Alto, Calif., pp. 71-77, 1973.

Linde, A.T., and M.J.S. Johnston, Source parameters of the October 1,1987, Whittier Narrows earthquake from crustal deformation data, *J. Geophys. Res.*, this issue.

Mansinha, L., and D.E. Smylie, The displacement fields on inclined faults, *Bull.Seismol. Soc. Am.*, 61, 1433-1440, 1971.

Mayer, L., Subsidence analysis of the Los Angeles Basin, in edited by R. Ingersoll and G. Ernst, *Cenozoic Basin Development of Coastal California*, Prentice-Hall, Englewood Cliffs, N.J. pp. 299-320, 1987.

Namson, J., and T. Davis, A structural transact of the western Transverse Ranges, California: Implications for lithospheric kinematics and seismic risk evaluation, *Geology*, 1b, 675-679 1988.

Stein, R.S., Discrimination of tectonic displacement from slope-dependent errors in geodetic leveling from southern California, 1953-1979, in *Earthquake Prediction: An International Review*, Maurice Ewing Ser. vol. 4, edited by D. W. Simpson and P. G. Richards, pp. 441-456, AGU, 1981.

Stein, R.S., and G.C.P. King, Seismic potential revealed by surface folding: 1983 Coalinga, California, earthquake, *Science*, 224, 869-872, 1984.

Stein, R.S., and W. Thatcher, Seismic and aseismic deformation associated with the 1952 Kern County, California, earthquake and relationship to the Quaternary history of the White Wolf fault, *J. Geophys. Res.*, 86, 4913-4928, 1981.

Stein, R.S., C.T. Whalen, S.R. Holdahl, W.E. Strange, and W. Thatcher, Saugus-Palmdale, California, field test for refraction error in historical leveling surveys, *J. Geophys. Res.*, 91, 9031-9044, 1986.

Stein, R.S., C.T. Whalen, S.R. Holdahl, W.E. Strange, and W. Thatcher, Reply, *J. Geophys. Res.*, 92, 10,715-10,717, 1987.

Stein, R.S., and R.S. Yeats, Hidden Earthquakes: Large earthquakes need not take place along faults that cut the earth's surface; they can also nucleate along "blind" faults beneath folded terrain, *Sci. Am.*, 260 (6), 1989.

Strange, W.E., The effect of systematic errors in geodynamic analysis, in *Proceedings of the 2nd International Symposium on Problems Related to the Redefinition of North American Vertical Datum*, pp.705-728, Onowa, Ont., 1980.

Sykes, L.R., and R.C. Quinmeyer, Repeat times of great earthquakes along simple plate boundaries, in *Earthquake Prediction: An International Review*, Maurice Ewing Ser. vol. 4, edited by D.W. Simpson and P. G. Richards, pp. 217-247, AGU, Washington D.C. 1981.

Truex, J.N.(Ed.), Tour of the oil fields of the Whittier fault zone, Los Angeles basin, California, *Pacific Sections Guideb*. 39, American Association of Petroleum Geologists, Los Angeles, Calif., 76 pp., 1975.

U.S. Geological Survey, Downey sheet, California (15' topographic quadrangle, surveyed 1893-1994), Reston, Va., 1896.

U.S. Geological Survey, Pomona sheet, California (15' topographic quadrangle, surveyed 1894), Reston, Va., 1897.

U.S. Geological Survey, Pasadena sheet, California (15' topographic quadrangle, surveyed 1894), Reston, Va., 1900.

U.S. Geological Survey, Anaheim sheet, California (15' topographic quadrangle, surveyed 1894), Reston, Va., 1901.

Yeats, R.S., Late Quaternary slip rate on the Oak Ridge fault, Transverse Ranges, California: Implications for seismic risk, *J .Geophys. Res.*, 93, 12,137-12,148, 1988.

Yerkes, R.F., Geologic and seismic setting, in *Evaluating Earthquake Hazards in the Los Angeles Region - An Earth Science Perspective*, edited by J.I. Ziony, *U.S. Geol. Surv. Prof Pap*, 1360, 347-374, 1985.

Yerkes, R.F., T.H. McCulloh, J.E. Schoellhamer, and J.G. Vedder, Geology of the Los Angeles Basin -An introduction, *U.S. Geol. Surv. Prof Pap*. 420-A, 57 pp.,1965.

Zepeda, R.L., and E.A. Keller, Rates of active tectonics at Wheeler Ridge anticline, So. San Joaquin Valley, California, *Geol. Soc. Am. Abstr.. Programs*, 18, 126,1986.

J. Lin, Department of Geology and Geophysics, Woods Hole Oceanographic Institution, Woods Hole, MA 02543.

R. S. Stein, U.S. Geological Survey, 345 Middlefield Road, MS977, Menlo Park, CA 94025.